Defense Technical Information Center Compilation Part Notice

ADP012227

TITLE: Thermal and Structural Characterization of Nanocomposite Iron Nitride - Alumina and Iron Nitride - Silica Particles

DISTRIBUTION: Approved for public release, distribution unlimited

This paper is part of the following report:

TITLE: Nanophase and Nanocomposite Materials IV held in Boston, Massachusetts on November 26-29, 2001

To order the complete compilation report, use: ADA401575

The following component part numbers comprise the compilation report:
ADP012174 thru ADP012259

Mat. Res. Soc. Symp. Proc. Vol. 703 © 2002 Materials Research Society V9.16

Thermal and Structural Characterization of Nanocomposite Iron Nitride - Alumina and Iron Nitride - Silica Particles

Ann M. Viano[1] and Sanjay R. Mishra[2]
[1]Department of Physics, Rhodes College, 2000 North Parkway
Memphis, TN 38112, U.S.A.
[2]Department of Physics, The University of Memphis,
Memphis, TN 38152, U.S.A.

ABSTRACT

Nanocomposite iron nitride based powders are known to have enhanced magnetic and other physical properties. To further explore their potential for application in various fields, we have performed a systematic study of the iron nitride - alumina and iron nitride - silica systems. Iron nitride powder of composition Fe_xN ($2 < x < 4$), containing both Fe_3N and Fe_4N phases, was mechanically milled with Al_2O_3 or SiO_2 powder for 4, 8, 16, 32, and 64 hours at the following compositions; $(Fe_xN)_{0.2}(Al_2O_3)_{0.8}$, $(Fe_xN)_{0.6}(Al_2O_3)_{0.4}$, $(Fe_xN)_{0.2}(SiO_2)_{0.8}$, and $(Fe_xN)_{0.6}(SiO_2)_{0.4}$. Differential thermal analysis and X-ray diffraction were performed to investigate thermal and structural transitions as a function of milling time. As the milling time is increased, the thermal peak corresponding to Fe_4N is diminished, while the one corresponding to Fe_3N is enhanced. These transitions are correlated with X-ray diffraction patterns. All XRD peaks broaden as a function of milling time, corresponding to smaller particle size. Transmission electron microscopy also reveals a decrease in particle size as the milling time in increased.

INTRODUCTION

Small magnetic particles are important in many practical applications for their superior magnetic properties such as high saturation magnetization and high coercive field. Improvements in these properties have been obtained through sputtering [1,2] and mechanical alloying [3] of iron particles with alumina or silica, an improvement which has been correlated with a reduction in particle size. Metal-metalloids, such as Fe_xN, have these desirable magnetic properties, but conventional techniques used to produce small particles often lead to oxidation and the formation of an iron oxynitride surface layer, which is ferromagnetically coupled to the core of a particle. Surface oxidation may be avoidable by embedding single domain Fe_xN particles in an insulating matrix such as Al_2O_3 or SiO_2. In fact, iron particles dispersed in such an insulating matrix have shown enhanced magnetic and mechanical properties [3-5]. In this work, small Fe_xN particles are embedded in an insulating matrix through mechanical ball-milling. The resulting particles should have the advantageous properties of both small particle size and metal-metalloid composition. To fully understand the mechanisms producing these particles, structural and thermal studies are performed in this study to evaluate the phase formation as a function of milling time.

EXPERIMENTAL DETAILS

Samples of iron nitride - alumina or iron nitride - silica were formed by mechanically milling powder of Fe_xN ($2<x<4$) with Al_2O_3 or SiO_2 powder for 4, 8, 16, 32, or 48 hours in a Fritsch planetary ball mill. The 325 mesh powders were 99.9% pure. Oxidation during milling was prevented by milling in the presence of ethyl alcohol. The mixture of Fe_xN powder to Al_2O_3 or SiO_2 powder was varied so that samples at each milling time were obtained for $(Fe_xN)_y(Al_2O_3)_z$ and $(Fe_xN)_y(SiO_2)_z$ with y = 0.2 and 0.8 (z = 0.8 and 0.2, respectively).

Thermal analysis was performed using an Instrument Specialists differential thermal analyzer with Pt/PtRd thermocouples and alumina sample and reference cups. Al_2O_3 powder was used as the reference material and scans were carried out with a heating / cooling rate of 10° / minute. Powder X-ray diffraction data was obtained with a Philips PC-APD3520 diffractometer using Cu K_α radiation. Samples were prepared for transmission electron microscopy (TEM) by sonicating the powder in methanol and then placing a few drops of the solution onto a holey-carbon coated grid. TEM was performed on a JEOL 1200 EX. TEM negatives were scanned at 1200dpi and then analyzed using the National Institute of Health's (NIH) Image software to measure particle size.

RESULTS AND DISCUSSION

Figure 1 shows XRD plots for the milled compounds with y = 0.2 (z = 0.8) and the pure Fe_xN powder. The starting Fe_xN powder ($2 < x < 4$) is a mixture of Fe_3N (ε phase) and Fe_4N (γ').

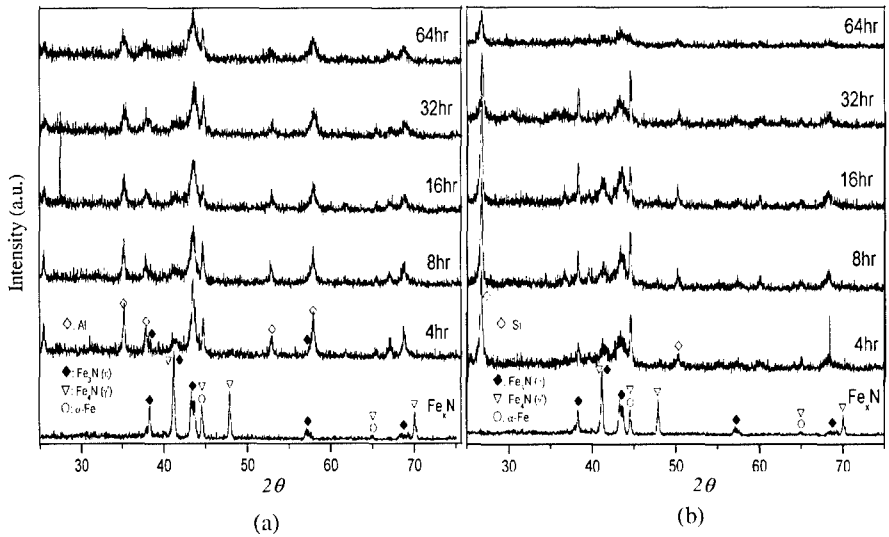

Figure 1: XRD patterns for (a) $(Fe_xN)_{0.2}(Al_2O_3)_{0.8}$ and (b) $(Fe_xN)_{0.2}(SiO_2)_{0.8}$ for the various milling times and for the starting Fe_xN powder.

The peaks at 44.5° and 65.0° could be either α-Fe or γ' –Fe_4N. For the Al_2O_3 series (figure 1a), it is clear that peaks corresponding to Fe_4N decrease in intensity with milling time. In particular, the Fe_4N peaks at 48° and 70° completely disappear at even short milling times. An increase in milling time also correlates with an increase in the intensity of the Fe_3N peaks, particularly those at 43.3° and 69°. This suggests that milling induces a transition from Fe_4N to Fe_3N. Thus, there is an excess of Fe, which is evidenced by the enhancement of α-Fe peaks at 44.5° and 65°. The peak at 41° (γ' and ε) grows on high side with milling time, which indexes more to the Fe_3N phase. A similar trend is seen for the SiO_2 series (figure 1b). The Fe_3N peaks increase in intensity while the peaks corresponding to the γ' phase decrease. Again, the persistence of the peak at 44° suggests a growth of α-Fe due to excess Fe coming from the Fe_4N to Fe_3N transition. Similar results were obtained for the higher Fe composition samples; $(Fe_xN)_{0.6}(Al_2O_3)_{0.4}$ and $(Fe_xN)_{0.6}(SiO_2)_{0.4}$. All of the XRD peaks broaden as milling time increases, indicates a decrease in particle size.

Figure 2 displays the DTA traces for both series as well as the curve for the starting Fe_xN powder. The ε phase (Fe_3N) has a wide range of solubility and its decomposition temperature at 25% N (atomic percent) occurs over a range of temperatures, but is less than 680°C for bulk material. Fe_4N, with a much narrower range of solubility, decomposes at 680°C for bulk material [6]. For small particles, these decompositions occur at lower temperatures. Decomposition temperatures of 570°C have been reported for 10μm Fe_3N particles [7], and 410°C-582°C has been reported for 0.3-5μm Fe_3N particles [8]. Table I displays our average

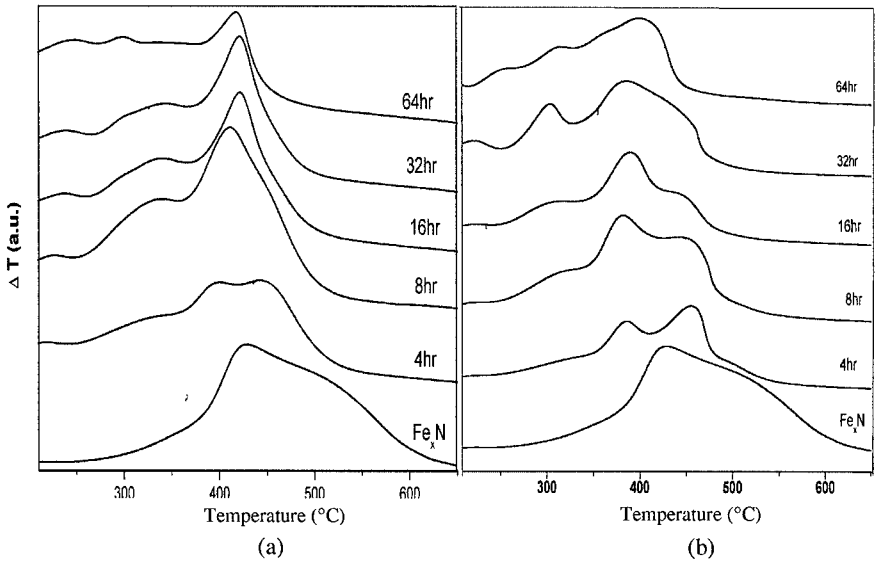

Figure 2: DTA curves for (a) the $(Fe_xN)_{0.2}(Al_2O_3)_{0.8}$ series and (b) the $(Fe_xN)_{0.6}(Al_2O_3)_{0.4}$ series. The y-axis is ΔT in °C, but normalized to show multiple curves on one graph. The peaks shown covered a range in ΔT of 20°C.

Table I Average particle size as measured by TEM studies for the Al_2O_3 samples.

Milling Time (hr)	Average Particle Size (nm)	
	$(Fe_xN)_{0.2}(Al_2O_3)_{0.8}$	$(Fe_xN)_{0.6}(Al_2O_3)_{0.4}$
4	376	516
8	278	340
16	172	232
32	159	200
64	64	110

particle sizes for the Al_2O_3 samples as measured by TEM. Since our particle sizes are all less than 0.5μm, the decomposition of the nitride phases will occur at lower temperatures. For the starting powder, which is a mixture of Fe_3N (ε) and Fe_4N (γ'), two exothermic peaks appear in range for nitride decomposition (400-600°C). The prominent peak at 425°C likely represents Fe_3N decomposition, and the peak nested in its high temperature shoulder represents the decomposition of Fe_4N.

For the Al_2O_3 samples, the Fe_3N peak becomes more prominent with milling time. This peak also shifts to slightly lower temperature, which correlates with the decrease in particle size upon increased milling time. This shows, as did the XRD data, the Fe_4N being converted to Fe_3N upon increased milling time. The DTA curves also show the growth of a peak between 300°C and 350°C as milling time increases. If the excess Fe is going into the α phase, as suggested by the XRD, this peak could correspond to a transition from γ' to α-Fe as N is liberated. Both of these phases have a wide range of solubility for N below 590°C. These lowest temperature peaks could also be due to adsorbed water or the presence of hydrocarbons in the samples, which were milled in ethyl alcohol to prevent oxidation. The two nitride phase peaks are most prominent in the samples with lower milling time (see the 4, 8, 16hr samples for $(Fe_xN)_{0.6}(Al_2O_3)_{0.4}$, figure 2b). As the milling time increases, the lower temperature peak is more prominent. The shift to lower temperature for the Fe_3N peak is also most prominent in the $(Fe_xN)_{0.6}(Al_2O_3)_{0.4}$ series, although these particles are larger on average than those in the $(FexN)_{0.2}(Al_2O_3)_{0.8}$ samples. The higher concentration of Al_2O_3 is therefore partly responsible for the decomposition of the nitride phases.

A similar trend is seen for the SiO_2 samples (figure 3). For the $(Fe_xN)_{0.2}(SiO_2)_{0.8}$ (figure 3a) series, it is clear that the peak corresponding to Fe_3N (400-450°C) grows with increasing milling time, indicating the presence of more Fe_3N phase. This trend is also see for the $(Fe_xN)_{0.4}(SiO_2)_{0.4}$ series (figure 3b), with the exception of the 64hr and perhaps the 4hr sample. In these two cases, the Fe_4N peak is more prominent. The three prominent peaks between 200°C and 375°C for the 64hr sample suggest that it may have oxidized or otherwise been contaminated. More studies should be performed to verify this suggestion.

CONCLUSIONS

We have explored ball milling of Fe_xN and an insulating component (alumina or silica) as a means of producing ultrafine Fe_xN particles. A reduction of the Fe_xN particle size is seen as

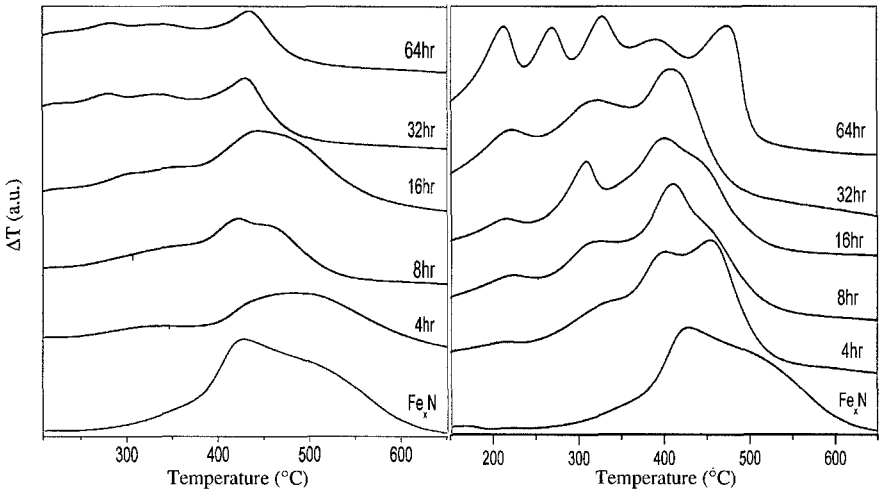

Figure 3: DTA curves for (a) the $(Fe_xN)_{0.2}(SiO_2)_{0.8}$ series and (b) the $(Fe_xN)_{0.4}(SiO_2)_{0.6}$ series. The y-axis is ΔT in °C, but normalized to show multiple curves on one graph. The peaks shown covered a range in ΔT of 20°C.

milling time increases, and this is accompanied by a transition from Fe_4N to Fe_3N. Both structural and thermal characterization show that there is an increase of the ε Fe_3N phase as milling time is increased. This decrease in size causes the decomposition of the Fe_3N phase to shift to a lower temperature, and a broadening of lines in the XRD spectra. Studies of the magnetic properties of these ultrafine particles have been completed [9] and suggest that ball milling iron nitride particles is a viable technique to produce small particles with desirable magnetic properties.

ACKNOWLEDGEMENTS

The authors would like to acknowledge Ms. Sharon Frase for her assistance with the electron microscopy performed in this study.

REFERENCENES

1. C. L. Chien in *Science and Technology of Nanostructured Magnetic Materials*, edited by G. C. Hadjipanayis and G. A Prinz, (Plenum, New York, 1991) p. 32.
2. B. Abeles in *Applied Solid State Science: Advances in Materials and Devices Research*, edited by R. Wolfe, (Academic, New York, 1976) p. 1.
3. A. Gavrin and C. L. Chien, *J. Appl. Phys.* **67**, 938 (1990).

4. A. K. Giri, C. De Julian, and J. M. Gonzalez, *J. Appl. Phys.* **76**, 6573 (1994).
5. T. E. Schlesinger, R. C. Cammarata, A. Gavrin, C. L. Chien, M. F. Ferber, and C. Hayzelden, *J. Appl. Phys.* **70**, 3275 (1992).
6. K. H. Jack, *J. Appl. Phys.* **76**, 6620 (1994).
7. G. M. Wang, S. J. Campbell, and W. A. Kaczmarek, *Mat. Sci. Forum* **235-238**, 433 (1997).
8. W. A. Kaczmarek and B. W. Ninham, *J. Mat. Sci.* **30**, 5514 (1995).
9. S. R. Mishra, G. J. Long, F. Grandjean, R. P. Hermann, S. Roy, N. Ali, and A. Viano, *J. Appl. Phys.* (in press).